

Journal Pre-proofs

Failure analysis of blades and vanes of a compressor for a gas turbine engine

Hyeok-Jun Kwon, Dooyoul Lee, Young-Kook Lee

PII: S1350-6307(21)00246-6

DOI: <https://doi.org/10.1016/j.engfailanal.2021.105386>

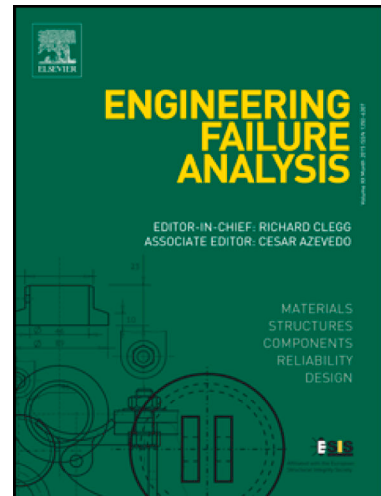
Reference: EFA 105386

To appear in: *Engineering Failure Analysis*

Received Date: 10 December 2020

Revised Date: 5 March 2021

Accepted Date: 18 March 2021



Please cite this article as: Kwon, H-J., Lee, D., Lee, Y-K., Failure analysis of blades and vanes of a compressor for a gas turbine engine, *Engineering Failure Analysis* (2021), doi: <https://doi.org/10.1016/j.engfailanal.2021.105386>

This is a PDF file of an article that has undergone enhancements after acceptance, such as the addition of a cover page and metadata, and formatting for readability, but it is not yet the definitive version of record. This version will undergo additional copyediting, typesetting and review before it is published in its final form, but we are providing this version to give early visibility of the article. Please note that, during the production process, errors may be discovered which could affect the content, and all legal disclaimers that apply to the journal pertain.

© 2021 Elsevier Ltd. All rights reserved.

Failure analysis of blades and vanes of a compressor for a gas turbine engine

Hyeok-Jun Kwon^a, Dooyoul Lee^{b,*}, Young-Kook Lee^{a,*}

^aDepartment of Materials Science and Engineering, Yonsei University, 03722 Seoul, Korea

^bDepartment of Defense Science, Graduate School of Defense Management, Korea National Defence

*Co-Corresponding author: phone 82-2-2123-2831, email yklee@yonsei.ac.kr

*Co-Corresponding author: phone 82-2-5089-1247, email dlee05291@gmail.com

Abstract

The flame-out occurred during the ground slide for take-off. As a result of immediate disassembly and inspection after failure, damages to blades and vanes were observed from the stage IV of a compressor. In particular, all stator vanes of stages IV and V, five rotor blades of stage V, and a rotor blade of stage VI were failed. In a fractured stator vane of stage IV, a fatigue-fracture surface, which was originated from the tip, appeared. However, the origin of fatigue cracking was not observed due to severe oxidation and wear. In the case of rotor blades at stages V and VI, the fatigue cracking was initiated from the nick damage part. The same nick damage was also observed in the stator vane of stage V, but fatigue cracking started from the convex surface. Comparing the microstructures of sound and fractured products showed that the convex surface of the fractured product had coarser grains compared to that of the sound product. This indicates that the coarse grains led to premature failure by fatigue cracking.

Keywords: Engine failure; Compressor stator vane failure; Fatigue failure; Coarse grain; IN 718

1. Introduction

A modern aviation gas turbine engine is an advanced technology complex consisting of compressor, combustion chamber, turbine, nozzle, and other modules. Among them, a compressor, which compresses a large amount of air and delivers it to a combustion chamber, plays an important role in the operation reliability of a gas turbine engine [1, 2]. The axial-compressor of the engine of a fixed-wing aircraft consists of a multi-stage rotor blades and stator vanes. All components are exposed to an environment where fatigue cracking is prone to occur due to a high level of repetitive stress generating during a high speed rotation for air compression [3]. Accordingly, most of the defects in compressor components are caused by high-cycle fatigue.

The fatigue failure of compressor components proceeds in an order of crack initiation, growth and final fracture due to repeated stress concentration after initial damage. The initial damage results from various factors [4-16], such as Foreign Object Damage (F.O.D), corrosion, friction, and notched shape. Fatigue cracks caused by F.O.D can be easily inferred in some cases because apparent damage from impact is observed at the crack initial site, and the chemical composition of impact object can be confirmed at the damage site [5, 6]. The corrosion is identified by the shape of a defect or corrosion products. Secondary cracks may occur around the fracture surface of a component, which suffered severe corrosion [7-9]. The friction leaves direct wear marks on the fracture surface, thermal damage caused by frictional heat, and friction cracks [10]. A notched shape is formed on the surface of the component due to damages generating during design or processing. A notch acts as a stress- concentrated site [11-13]. Because of the characteristic of each factor mentioned above, it is considered to be easy to determine the cause of initial damage. However, in reality, it is difficult to identify an initial damage due to the secondary damage occurring immediately after failure, in particular in the

case of a harsh operating environment.

Whereas the initial damage listed above are caused by external factors, fatigue properties of a component may be deteriorated by internal defects of a material, such as precipitates, inclusions, inhomogeneous grain size, etc. [14, 15]. The material defects are difficult to find, and even if discovered, it is difficult to take measures to prevent failure.

In the present study, the cause of engine flame-out resulting from compressor failure during take-off run was examined. The initial fracture occurred at the stage IV stator vane of a compressor consisting of eight stages. Damage was observed at rotor blades and stator vanes at stages from IV to VIII. To analyze the cause of engine failure, fractographic analysis was performed. In particular, the microstructure of a stator vane, which was failed by the surface damage generating from oxidation and abrasion, was deeply analyzed.

2. Experimental procedure

Damages were observed at all stages from the stage IV of a compressor to a combustion chamber. Among them, vanes of the stage IV, blades and vanes of the stage V, and blades of the stage VI were fractured and collected for examination. All fractured parts were cleaned using ethanol and acetone before analysis.

Although the chemical composition analysis was not performed, production specifications informed that the stator vane and the rotor blade were made of Inconel 718 and Ti-6Al-4V alloy, respectively.

Specimens were taken from the damaged vanes of stages IV and V using a wire saw. For comparison, several specimens were fabricated at the same stages of a sound (i.e. unfractured) product. The microstructures of specimens were observed using an optical microscope (OM; Nikon, MM-400) and a scanning electron microscope (SEM; HITACHI S-3700N) equipped

with an electron back-scattered diffractometer (EBSD; EDAX-TSL, Digiview). Whereas samples for optical observation were mechanically polished and etched with the Marble's etchant, samples for SEM-EBSD observation were mechanically polished using a suspension including 1 µm diamond particles, and then electrochemically polished using a mixed solution of 90% glacial acetic acid (CH_3COOH) and 10% perchloric acid (HClO_4) at 15 V for 1 min to remove the damaged layer. The accelerating voltage, probe current, working distance, and step size for SEM-EBSD operation were 20 kV, 15 nA, 15 mm, and 150 nm, respectively.

3. Result

3.1. Macroscopic observation

The engine failure occurred during take-off run. When the compressor was disassembled, it was readily found that rotor blades at stages V-VIII were damaged (Fig. 1a). However, the damage of stator vanes was difficult to be observed until the stator vane assembly in Fig. 1b was disassembled. Finally, severe damages were found from stage IV (Figs. 2a and c) after the dismantlement of the stator vane assembly. In particular, a vane at stage IV and a vane at stage V, five blades at the stage V and a blade at the stage VI were fractured. Regarding the stage IV, the trailing edge (TE) region of a vane was fractured with a size of $\sim 5 \text{ mm} \times \sim 32 \text{ mm}$ (Fig. 2a), and the other vanes had only nick damages. The blades at stages V and VI were fractured at different positions (Fig. 2b). Moreover, nick damages were observed in leading edge (LE) and TE regions. As seen in Fig. 2c, the vane of the stage V was fractured at the position of 13 mm away from the outer-platform part, and damages were observed in the TE region. Damages were also observed in the TE region of the other vanes of the stage V.

3.2. Microscopic observation

3.2.1. Stator vane at stage IV

The fractography of the fractured vane at the stage IV was performed (Fig. 2a). Severe oxidation and abrasion were observed throughout the fracture surface (Fig. 3a). No information was obtained due to abrasion at the tip (Fig. 3b). At a location 6 mm away from the tip, fatigue cracks started from each side of concave and convex parts (Fig. 3c); fatigue striations (yellow arrows in Fig. 3c) were observed at some fractured surfaces. Moreover, overload fractured surfaces were observed at the last stage of general fatigue cracking and the fractured surface exhibited a dimple structure (Fig. 3d). This observation indicates that cracking started from the tip and grew diagonally to the outer-platform and TE.

3.2.2. Rotor blade of stage V

Regarding the rotor blade at the stage V, nick damages were observed in LE and TE regions (Fig. 4a). Clear fatigue striations were not observed on the fractured surface at the SEM images. However, a beach mark which formed from LE towards TE, was observed at the OM images (Fig. 4b). This is indicative of the occurrence of fatigue cracking. The damaged part of the LE region exhibited a dimple structure, i.e., a trace of overload fracture (Fig. 4c). In addition, the SEM-EDXS result (Fig. 4d) shows that the LE region of the blade possesses the same chemical elements (Ni, Cr and Nb) with main chemical elements of the vane. This indicates that the initial damage in LE was caused by vane fragment. That result was observed in five blades of stage V and a blade of stage VI.

3.2.3. Stator vane of stage V

The vane of the stage V was completely fractured unlike the stator of stage IV, where a

part of airfoil was fractured and nick damages were observed only at the trailing edge (Fig. 2c). The Fig. 5 shows the fractured surface of the failed vane of the stage **V**. As shown in Fig. 5b, the fatigue crack was initiated and propagated from the center of the convex surface, not from the damaged part of TE (Red arrow in the fig. 5a). The direction of fatigue cracking was determined by the formation of fatigue striations (Figs. 5c-e). The main chemical elements of the blade, such as Ti, Al and V, were detected at the damaged part of the vane (Fig. 5f).

3.2.4. Microstructural analysis of Stator vanes at stages IV and V

Except for the blades at stages **V** and **VI**, in which fatigue cracks caused by nick damages are clearly observed, microstructures of the vanes at stages **IV** and **V** were observed. Compared with the sound vane (i.e., unfractured vane) of stage **IV**, both fractured (Fig. 6a) and sound (Fig. 6b) vanes revealed no significant differences in grain size and precipitate fraction (Fig. 7), which could affect fatigue cracking. Meanwhile, some defects were observed at the surface of concave and tip near the fracture surface (blue circles in Figs. 6c and d). The cross-sectional shape of the surface defect is similar to a typical shape of a corrosion pit. The oxygen was detected near the defect by the SEM-EDXS analysis although the measured oxygen content (~8 wt.%) is less than the oxygen content (> 15 wt.%) measured from corrosion pits in literature [17, 18]. This is probably because the size of the defect observed in the present study was so small that the chemical composition of a matrix or a resin near the defect was measured together.

Fig. 8 exhibits microstructures of sound (Fig. 8a) and fractured (Fig. 8b) vanes of stage **V**. Both vanes revealed a similar fraction of precipitates (Fig. 7), but different grain sizes. In particular, the fractured vane possessed coarse grains in the convex surface. To evaluate the distribution of grain size, SEM-EBSD observation was performed (Fig. 9). As a result, the

grain size of the sound vane (Figs. 9a and b) was finer than that of the fractured vane (Figs. 9c and d).

4. Discussion

Based on the results mentioned above, it was realized that the flame-out of the gas turbine engine stemmed mainly from internal object damage (I.O.D) caused by the fracture of the stator vane of stage **IV**. However, since the initiation point of fatigue cracking was completely contaminated by wear and oxidation, it was difficult to elucidate the root cause of fracture. Nevertheless, based on failure cases [7-9, 19-21], it can be deduced that the compressor vane of the gas turbine engine might be fractured by corrosion. Corrosion is a typical cause of damage occurring at various parts of aircraft, and can serve as a starting point for fatigue cracking. In the present study, micro-corrosion (i.e., pitting) was also observed at the tip of the vane of stage **IV** (Fig. 6). Another cause of fracture is dispersion of material strength. Even if all materials undergo heat treatment and manufacture process under complete control, the inhomogeneity of material properties may exist. Furthermore, mechanical properties may also change depending on the environment that the material is exposed to [22].

Regarding the blades of stages **V** and **VI**, the damages of LE and TE were confirmed, and the fatigue crack was propagated from the damaged part of LE (Fig. 4). The SEM-EDXS result exhibited that the LE parts of blades were damaged by broken fragments of vanes. Accordingly, it is considered that the damaged LE parts provided stress concentration sites and the origin of fatigue cracking. Fatigue cracks, caused by stress concentration at the damaged part, are frequently reported in many previous studies [5, 23].

Considering the stage and location of the compressor, the fracture of the stage **V** vane is most likely due to the secondary damage caused by fragments of vanes of stage **IV** and blades

of stage **V**. However, even if the vane of stage **IV** did not break, the possibility of engine damage is thought to be high because the vane of stage **V** had fatigue cracks (Fig. 5). The reason is that the initiation site of fatigue cracking was not the location where nick damage was observed. The cause of the fatigue crack is considered to be due to coarse grains present in the convex surface (Figs. 8 and 9). Abikchi *et al.* [24] reported that fatigue cracking started primarily from coarse grains in Inconel 718 and experimentally showed that Inconel 718 with coarse grains possessed the lower cycle for the start of fatigue cracking. The possibility of fatigue cracking increases due to the low fraction of Γ'' precipitates within coarse grains and irregular distribution of slip bands [25]. In addition, Inconel 718 is known to follow the Hall-Petch theory, where the strength increases with grain refinement [26]. In other words, fatigue properties deteriorated due to coarse grain formation on convex surface of the vane. Meanwhile, coarse grains on the surface form during heat treatment and manufacturing process [27, 28].

5. Conclusions

- a. The cause of fatigue cracking in the stator vane of stage **IV** was not confirmed due to the severe contamination of the crack origin. However, corrosion is considered to be the cause of cracking due to the presence of corrosion pits observed on the surface of airfoil.
- b. The rotor blades of stages **V** and **VI** were failed by fatigue cracking that was initiated at the damaged part. The chemical elements of the vane were detected at the damaged part of rotor blades. This implies that the damages of rotor blades were caused by the fragments of the vane.
- c. The stator vane of stage **V** was failed by fatigue cracking, which was initiated at the middle part of the convex surface, not the nick damage part. Compared with the sound

vane, the fractured vane possessed coarser grains at the convex surface. It is deduced that coarse grains are the main cause of fatigue cracking.

6. Acknowledgement

The authors thank Ms. Shon at ATRI(Aero Technology Research Institute, Republic of Korea Air Force) for her technical assistance of SEM work.

References

- [1] Cohen H., Rogers G.F.C., Saravanamuttor H.I.H., Gas turbine theory, Longman Scientific & Technical, New York, 1987.
- [2] Greatrix D.R., Gas Turbine Engines Fundamentals. In Powered Flight. Springer, London, 2012.
- [3] B.A. COWLES, High cycle fatigue in aircraft gas turbines - an industry perspective, Int. J. Fract. 80 (1996) 147-163. <https://doi.org/10.1007/BF00012667>.
- [4] Tim J Carter, Common failure in gas turbine blades, Eng. Fail. Anal. 12 (2005) 237-247. <https://doi.org/10.1016/j.engfailanal.2004.07.004>.
- [5] E. Silveira, G. Atxaga, A.M. Irisarri, Failure analysis of two sets of aircraft blades, Eng. Fail. Anal. 17 (2010) 641-647. <https://doi.org/10.1016/j.engfailanal.2008.10.015>.
- [6] Zhenhua Zhao, Lingfeng Wang, Kainan Lu, Yongjian Li, Wei Chen, Lulu Liu, Effect of foreign object damage on high-cycle fatigue strength of titanium alloy for aero-engine blade, Eng. Fail. Anal. 118 (2020) 10482. <https://doi.org/10.1016/j.engfailanal.2020.104842>.
- [7] Amir Masoud Mirhosseini, S. Adib Nazari, A. Maghsoud Pour, S. Etemadi Haghghi, M. Zareh, Failure analysis of first stage nozzle in a heavy-duty gas turbine, Eng. Fail. Anal. 109 (2020) 104303. <https://doi.org/10.1016/j.engfailanal.2019.104303>.
- [8] L. Witek, M. Wierzbinska, A. Poznanska, Fracture analysis of compressor blade of a helicopter engine, Eng. Fail. Anal. 16 (2009) 1616-1622. <https://doi.org/10.1016/j.engfailanal.2008.10.022>.
- [9] A. Mokaberi, R. Derakhshandeh-Haghghi, Y. Abbaszadeh, Fatigue fracture analysis of gas turbine compressor blades, Eng. Fail. Anal. 58 (2015) 1-7. <https://doi.org/10.1016/j.engfailanal.2015.08.026>.
- [10] Bok-Won Lee, Jungjun Suh, Hongchul Lee, Tae-gu Kim, Investigations on fretting fatigue

in aircraft engine compressor blade, Eng. Fail. Anal. 18 (2011) 1900-1908.
<https://doi.org/10.1016/j.engfailanal.2011.07.021>.

[11] Ehsan Masoumi Khalil Abad, G.H.Farrahi, Mahdi Masoumi Khalil, Amir Ahmad Zare, Siavash Parsa, Failure Analysis of a Gas Turbine Compressor in a Thermal Power Plant, J. Fail. Anal. Prev. 13 (2013) 313-319. <https://doi.org/10.1007/s11668-013-9663-8>.

[12] Swati Biswas, MD Ganeshachar, Jivan Kumar, VN Satish Kumar, Failure Analysis of a Compressor Blade of Gas Turbine Engine, Procedia Eng. 86 (2014) 933-939.
<https://doi.org/10.1016/j.proeng.2014.11.116>.

[13] Mingchao Ding, Yuanliang Zhang, Huitian Lu, Yuan Sun, Numerical investigation on stress concentration of surface notch on blades, Eng. Fail. Anal. 122 (2021) 105241.
<https://doi.org/10.1016/j.engfailanal.2021.105241>.

[14] Wassim Maktouf, Kacem Saï, An investigation of premature fatigue failures of gas turbine blade, Eng. Fail. Anal. 47 (2015) 89-101. <https://doi.org/10.1016/j.engfailanal.2014.09.015>.

[15] Qiaoling Chu, Min Zhang, Jihong Li, Failure analysis of impeller made of FV520B martensitic precipitated hardening stainless steel, Eng. Fail. Anal. 34 (2013) 501-510.
<https://doi.org/10.1016/j.engfailanal.2013.07.003>.

[16] R. Chaharlang, E. Hajjari, S.M. Lari Baghal, M. Siahpoosh, Premature damage of the second stage nozzle guide vanes of a gas turbine made of Inconel 738LC, Eng. Fail. Anal. 105 (2019) 803-816. <https://doi.org/10.1016/j.engfailanal.2019.07.053>

[17] Jiand Miao, Qiang Wang, Corrosion rate of API 5L Gr. X60 multipurpose steel pipeline under combined effect of water and crude oil, Met. Mater. Int. 22 (2016) 797-809.
<https://doi.org/10.1007/s12540-016-6175-6>.

[18] Hai-xuan Yu, Xiao-lei-Xu, Zhi-wei Yu, Pitting-corrosion on internal wall of tee-pipe joined with main-pipe for seawater tank-washing system of a tanker, Eng. Fail. Anal. 104 (2019)

- 439-447. <https://doi.org/10.1016/j.engfailanal.2019.06.013>.
- [19] S.A. Barter, L. Molent, Fatigue cracking from a corrosion pit in an aircraft bulkhead, Eng. Fail. Anal. 39 (2014) 155-163. <https://doi.org/10.1016/j.engfailanal.2014.01.020>.
- [20] Kimberli Jones, David W. Hoeppner, Prior corrosion and fatigue of 2024-T3 aluminum alloy, Corros.Sci. 48 (2006) 3109-3122. <https://doi.org/10.1016/j.corsci.2005.11.008>.
- [21] G.S. Chen, K.-C. Wan, M. Gao, R.P. Wei, T.H. Flournoy, Transition from pitting to fatigue crack growth-modeling of corrosion fatigue crack nucleation in a 2024-T3 aluminum alloy, Mater. Sci. Eng. A. 219 (1996) 126-132. [https://doi.org/10.1016/S0921-5093\(96\)10414-7](https://doi.org/10.1016/S0921-5093(96)10414-7).
- [22] Tatsuo SAKAI, Masaki NAKAJIMA, Keiro TOKAJI, Norihiko HASEGAWA, Statistical distribution patterns in mechanical and fatigue properties of metallic materials, Mater. Sci. Res. Int. 3 (1997) 63-74. https://doi.org/10.2472/jsms.46.6Appendix_63.
- [23] Myounggu Park, Young-Ha Hwang, Yun-Seung Choi, Tae-Gu Kim, Analysis of a J69-T-25 engine turbine blade fracture, Eng. Fail. Anal. 9 (2002) 593-601. [https://doi.org/10.1016/S1350-6307\(02\)00003-1](https://doi.org/10.1016/S1350-6307(02)00003-1).
- [24] Meriem Abikchi, Thomas Billot, Jérôme Crépin, Arnaud Longuet, Caroline Mary, Thilo F. Morgeneyer, André Pineau, Fatigue life and initiation mechanism in wrought Inconel 718 DA for different microstructure, 13th International Conference in Fracture. (2013).
- [25] D. D. Krueger, Stephen D. Antolovich, R. H. Van Stone, Effects of Grain Size and Precipitate Size on the Fatigue Crack Growth Behavior of Alloy 718 at 427, Metall. Trans. A. 18 (1987) 1431-1449. <https://doi.org/10.1007/BF02646657>.
- [26] Muhammad Moiz, The influence of grain size on the mechanical properties of Inconel 718, Linköping University, Sweden (2013).
- [27] Richard Watson, Michael Preuss, Joao Quinta da Fonseca, Thomas Witulski, Gregor

Terlinde, and Markus Buscher, Characterization of abnormal grain coarsening in Alloy 718,
MATEC Web of Conferences. 14 (2014) 07004.
<https://doi.org/10.1051/matecconf/20141407004>.

[28] Chuya Aokia, Tomonori Ueno, Takehiro Ohno, Katsunari Oikawa, Influence of hot-working conditions on grain growth of superalloy 718, J. Mater. Process. Technol. 267 (2019) 26-33. <https://doi.org/10.1016/j.jmatprotec.2018.12.002>.

Figure caption list

Fig. 1. Damaged compressor part of (a) rotor blade assembly and (b) stator vane assembly.

Fig. 2. Fractured and damaged components of (a) Stator vanes of stage IV, (b) rotor blades of stages V and VI, and (c) stator vanes of stage V.

Fig. 3. (a) OM image of the entire fractured surface of a stator vane of stage IV. Magnified SEM images of (b) tip, (c) middle and (d) outer-platform parts corresponding to red boxes in (a). Yellow arrows indicate fatigue striations.

Fig. 4. Fractured surface of a rotor blade of stage V: OM images of (a) the entire fractured surface and (b) the middle part corresponding to red boxes in (a). Dotted yellow lines in (b) indicate the beach mark. (c) SEM image of the surface fractured by nick damage, and EDXS patterns of (d) nick-damaged area (LE side).

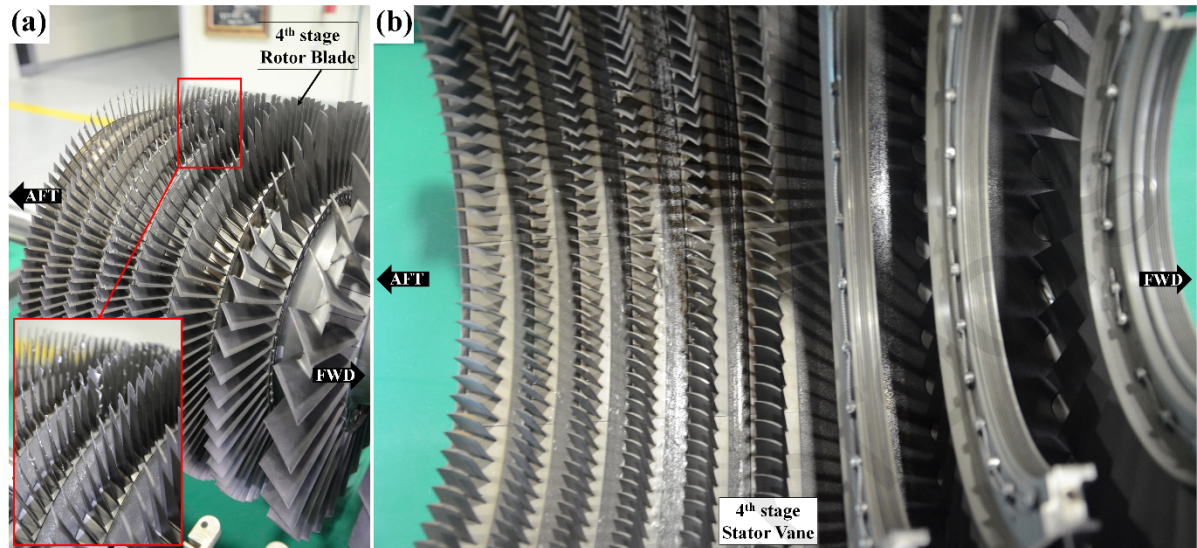
Fig. 5. (a) SEM image of a fractured stator vane of stage V. (b) Magnified SEM image of fractured surface corresponding to a red box in (a). (c-e) Magnified SEM images of fractured surface corresponding to red boxes in (b). Yellow arrows indicate the direction of fatigue crack propagation. (f) EDXS pattern of nick-damaged area on the fractured surface of the vane.

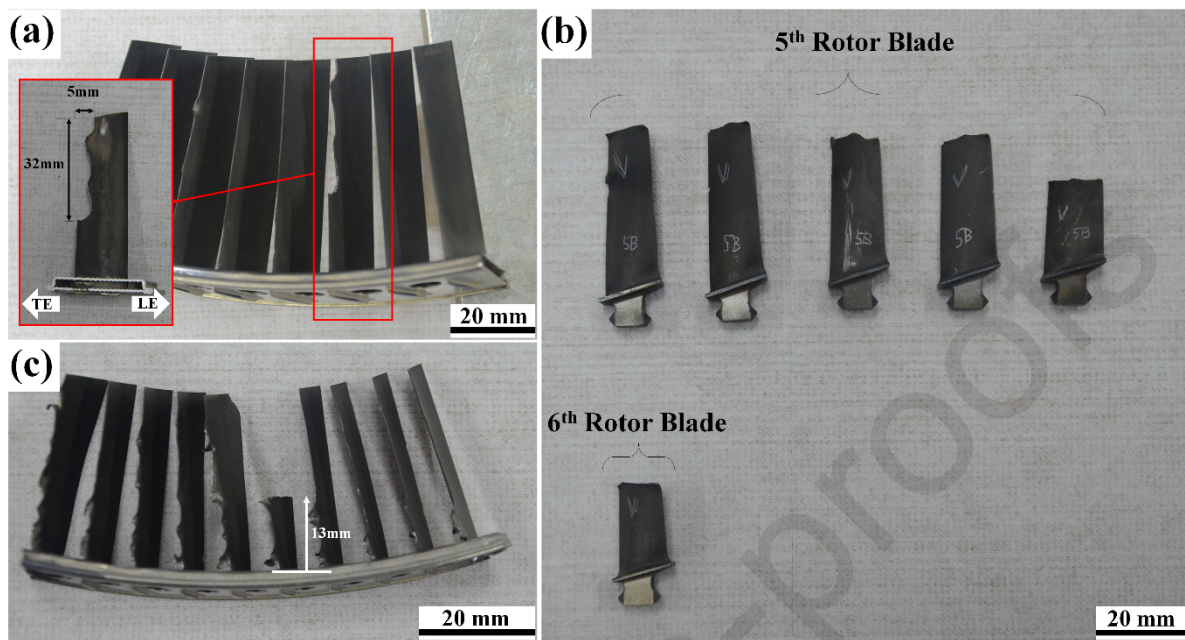
Fig. 6. OM images of (a) sound and (b) fractured stator vanes observed from a leading edge direction. (c, d) OM images showing the vicinity of the tip of the fractured vane.

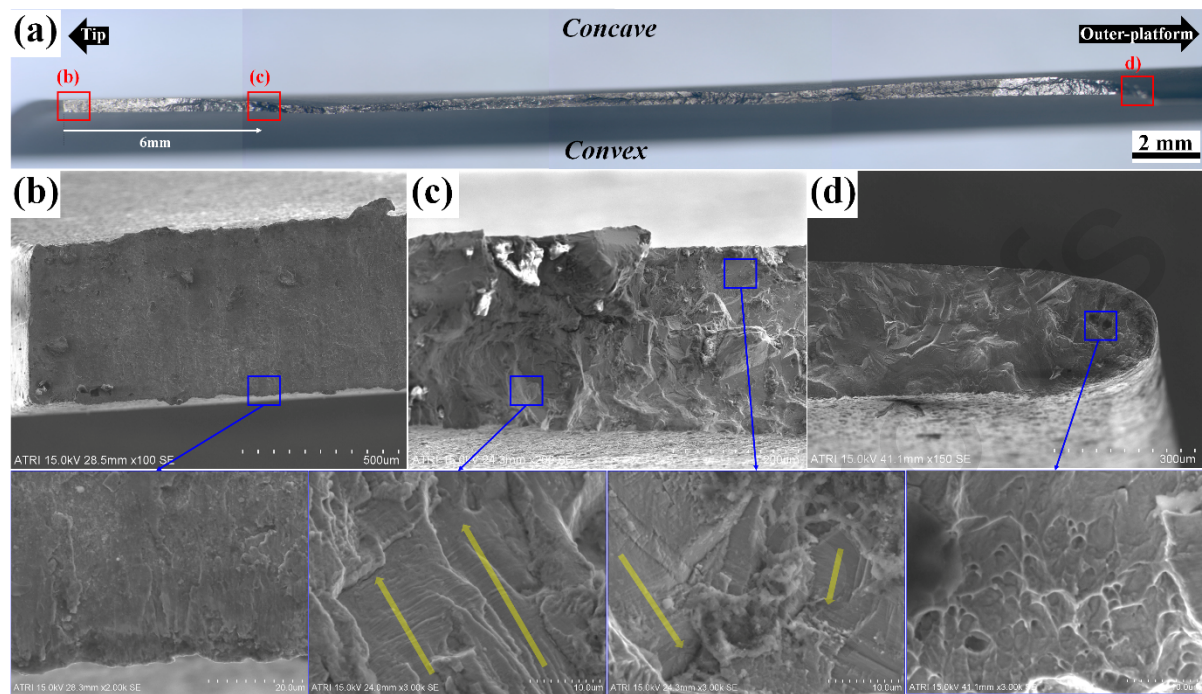
Fig. 7. The fractions of precipitates measured at fractured and sound vanes in the stage IV and V.

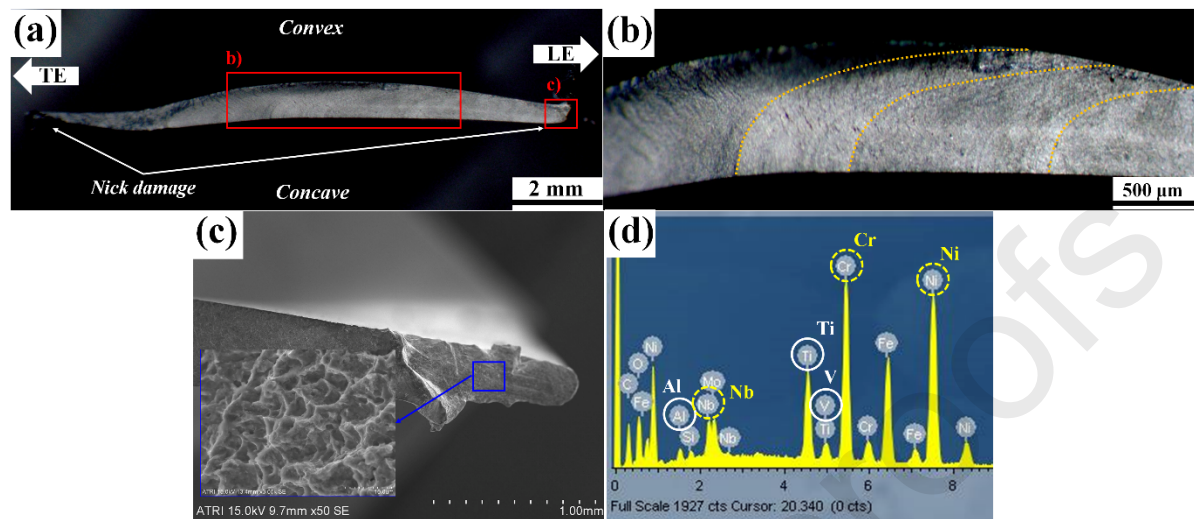
Fig. 8 OM images of (a) sound and (b) fractured stator vanes observed from the tip direction.

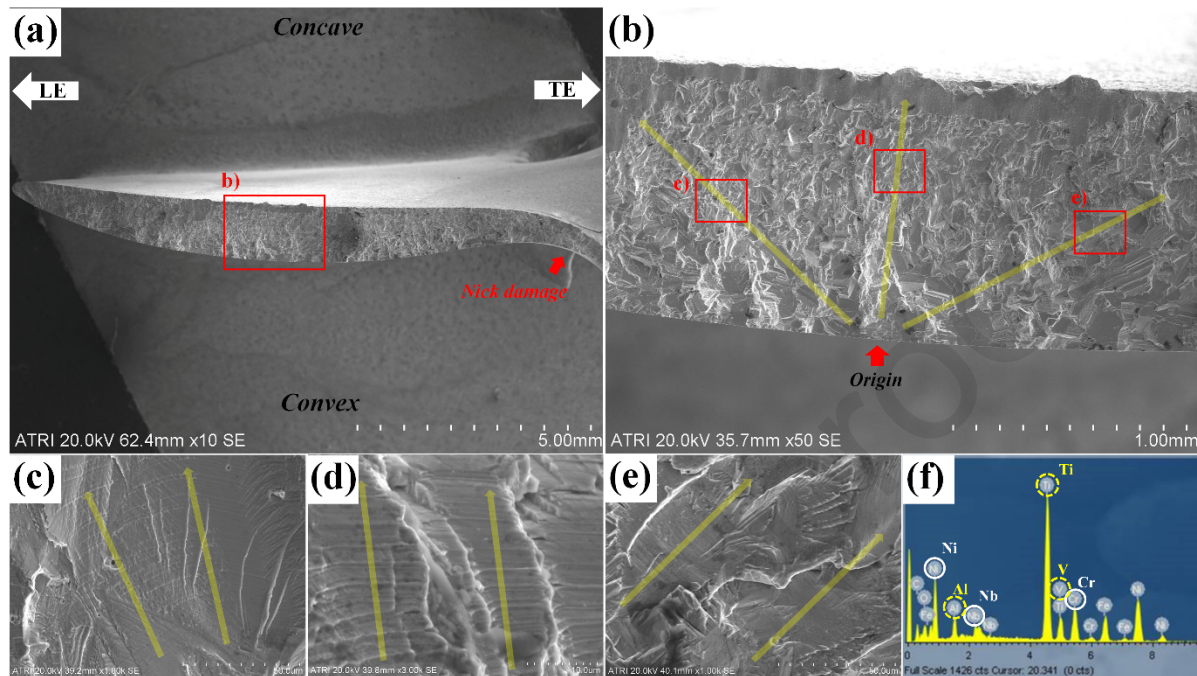
Fig. 9. (a, c) EBSD image quality (IQ) maps and (b, d) distribution of grain size: (a, b) sound and (c, d) fractured vanes. Blue lines are low-angle boundaries with misorientation angles of 3° - 15° . Black lines are high-angle boundaries with misorientation angles exceeding 15° .

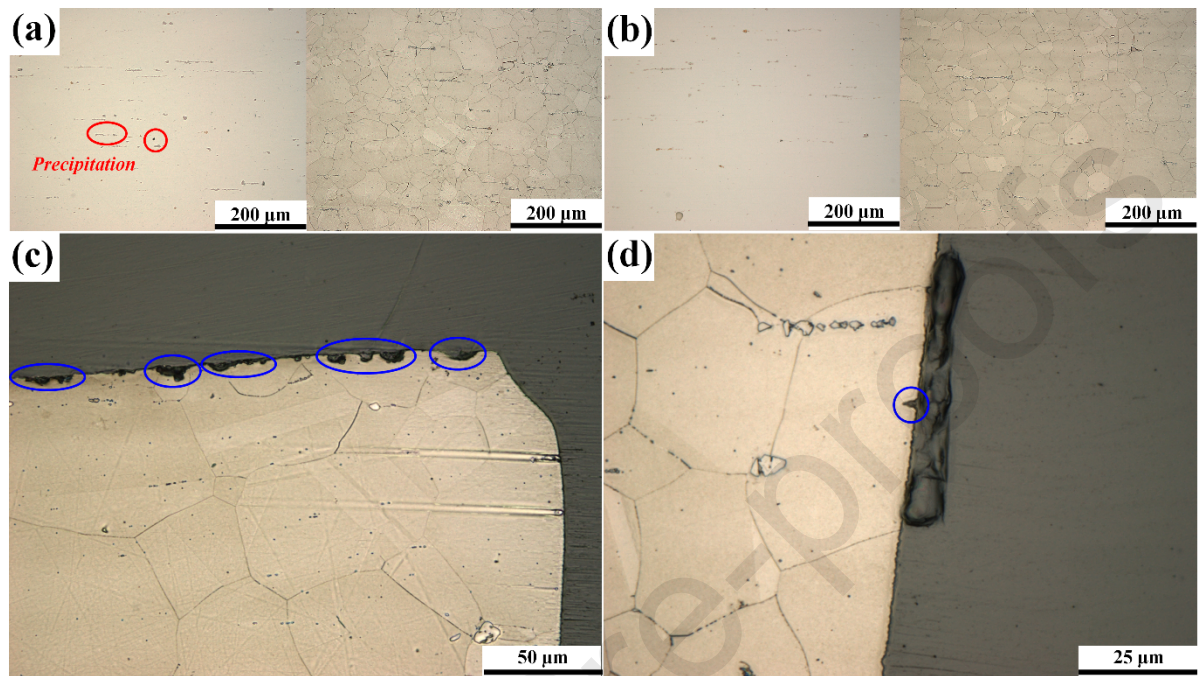


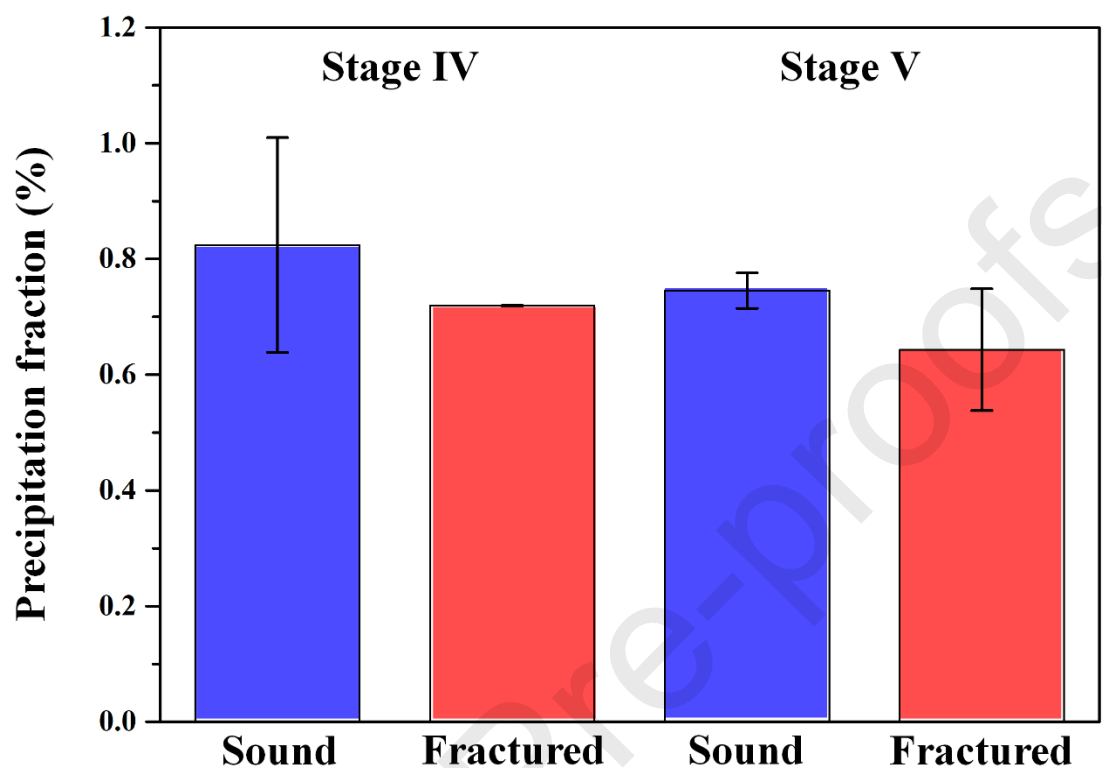


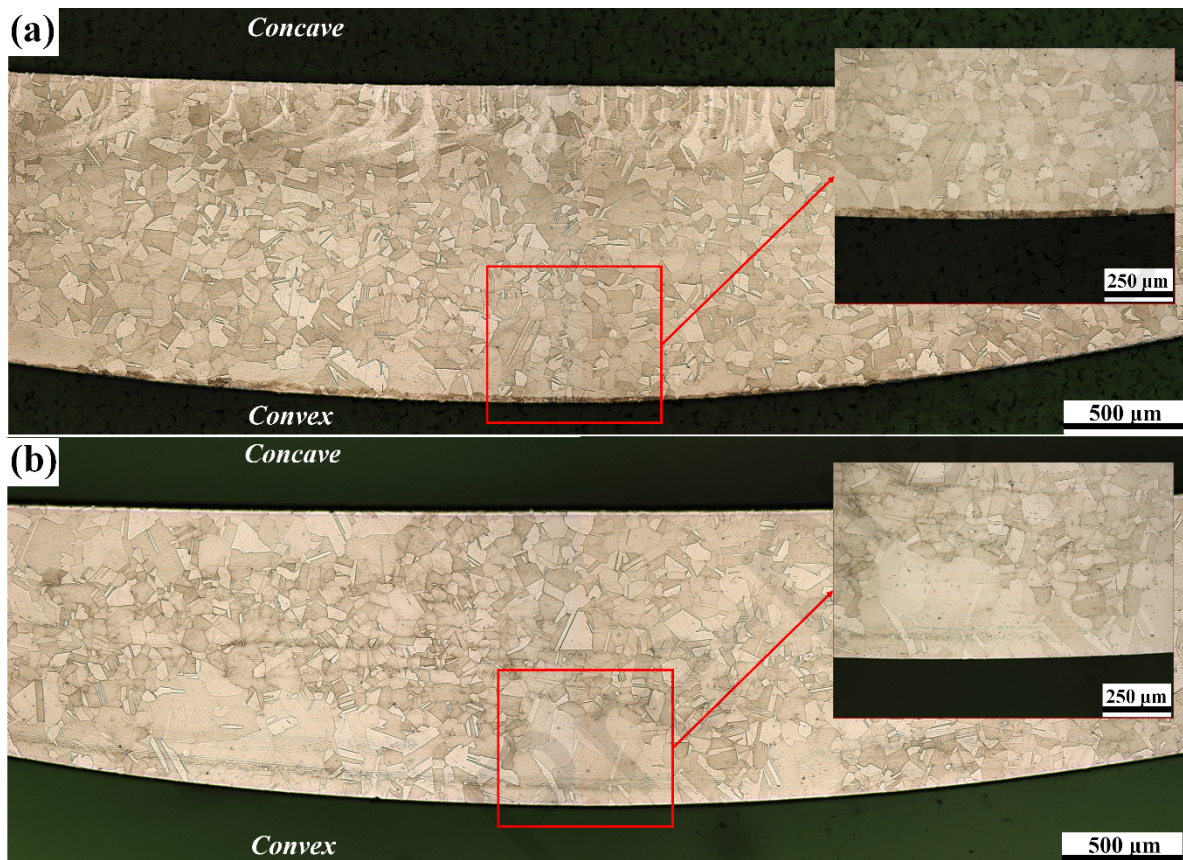


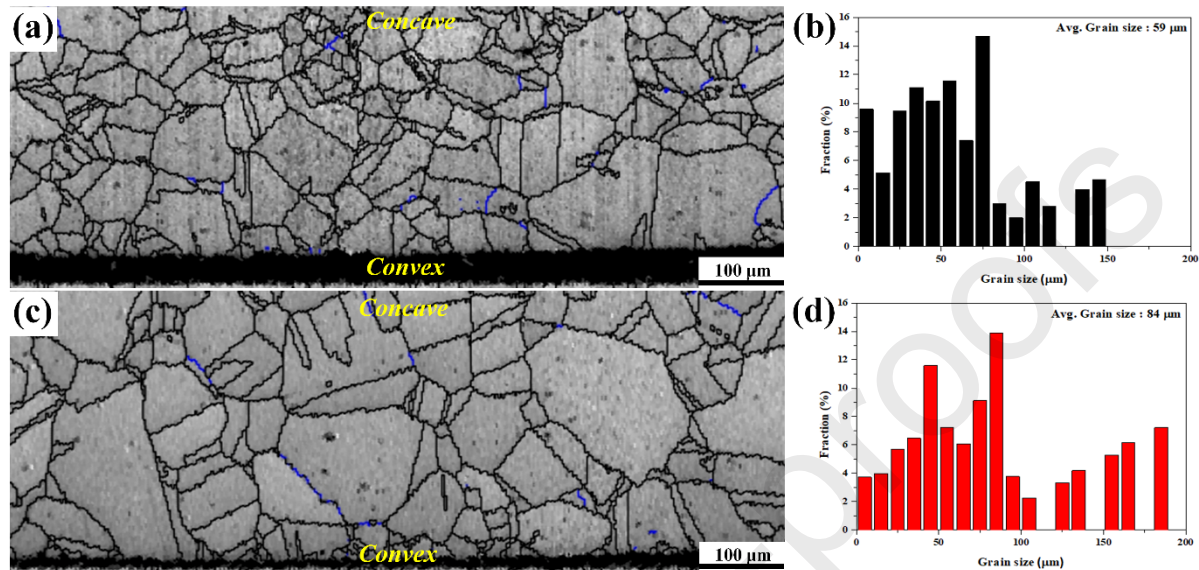


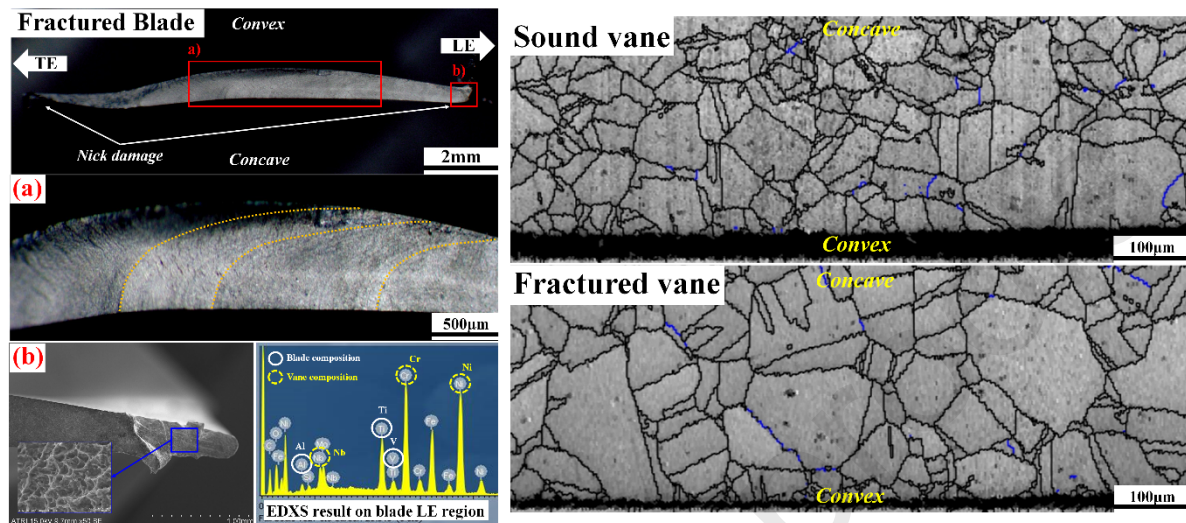












Highlight

- Failure analysis of a compressor for an aircraft gas turbine engine was conducted.
- Corrosion pits were observed in fractured vanes at the stage **IV** of the compressor.
- Coarse grains in the fractured vanes of stage **V** were observed through OM and EBSD.
- Fatigue properties of vanes were degraded by coarse grains.
- Fatigue cracks of blades were generated due to damages caused by vane fragments.

Declaration of interests

The authors declare that they have no known competing financial interests or personal relationships that could have appeared to influence the work reported in this paper.

The authors declare the following financial interests/personal relationships which may be considered as potential competing interests:

